Solar-Terrestrial Physics. 2022. Vol. 8. Iss. 4. P. 89–94. DOI: 10.12737/stp-84202209. © 2022
V.I. Sivtseva, P.P. Ammosov, G.A. Gavrilieva, A.M. Ammosova, I.I. Koltovskoi. Published by INFRA-M Academic Publishing House

UDC 550.388
DOI: 10.12737/stp-84202209

Received July 08, 2022
Accepted October 28, 2022

WAVE ACTIVITY OF THE MESOSPHERE IN THE PLANETARY WAVE RANGE ACCORDING TO OH (3-1) EMISSION OBSERVATIONS AT MAIMAGA AND TIKSI STATIONS FOR 2015–2020

V.I. Sivtseva
Yu.G. Shafer Institute of Cosmophysical Research and Aeronomy SB RAS,
Yakutsk, Russia, verasivtseva@gmail.com

P.P. Ammosov
Yu.G. Shafer Institute of Cosmophysical Research and Aeronomy SB RAS,
Yakutsk, Russia, ammosov@ikfia.ysn.ru

G.A. Gavrilieva
Yu.G. Shafer Institute of Cosmophysical Research and Aeronomy SB RAS,
Yakutsk, Russia, gagavrilyeva@ikfia.ysn.ru,
Institute of Solar-Terrestrial Physics SB RAS, Irkutsk, Russia

A.M. Ammosova
Yu.G. Shafer Institute of Cosmophysical Research and Aeronomy SB RAS,
Yakutsk, Russia, ammosovaam@mail.ru

I.I. Koltovskoi
Yu.G. Shafer Institute of Cosmophysical Research and Aeronomy SB RAS,
Yakutsk, Russia, koltigor@mail.ru

Abstract. The article compares the interannual variability of the atmosphere at the OH glow height, which can be associated with planetary wave propagation, at stations spaced in latitude. As a characteristic reflecting planetary wave activity we consider standard deviations of the average overnight temperature σ_{pw} from its monthly average after taking into account the seasonal variation. Joint mesopause temperature measurements at high latitudes at two optical stations Maimaga (63.04° N, 129.51° E) and Tiksi (71.58° N, 128.77° E) began in 2015. The stations are equipped with identical Shamrock (Andor) high image quality infrared spectrographs for registration of OH (3-1) in the near infrared region (~1.5 μm). The main result of studying the planetary wave activity during the 5-year period of simultaneous observations is that at Tiksi station it slightly (by about 1–2 K) exceeds that at Maimaga station. In average annual activity fluctuations, the presence of quasi-biennial oscillations is traced.

Keywords: planetary waves, mesopause region, hydroxyl.

INTRODUCTION

The term “planetary waves” (PW) describes wave disturbances of various types in the atmosphere, which have a global, planetary scale. Sources of their generation can be surface inhomogeneities, temperature contrast due to land and sea heating inhomogeneity, lunar gravitational tides, large-scale meteorological disturbances, etc. The dominant disturbances in the winter stratosphere and mesosphere are Rossby waves excited in the atmosphere by the latitudinal gradient of the Coriolis force, which balances pressure gradient changes [Smith, 2012; Yiğit, Medvedev, 2015]. Planetary waves are considered an important driver of meridional atmospheric circulation [Holton et al., 1995], which, due to its global nature, determines the dynamic coupling between different atmospheric layers. Moreover, breaking of planetary waves propagating upward from the troposphere can cause a sudden stratospheric warming in winter [Matsuno, 1971; Schoeberl, 1978].

There are two PW types: stationary (or quasi-stationary) and traveling. In the lower and middle atmosphere, stationary PWs are confined to a particular location, and their manifestations are difficult to separate from the background values of measured parameters during ground observations of the upper atmosphere. In [Smith, 2012], it is mentioned that the amplitude of such waves in the mesopause region (~100 km) is low. Thus, it is assumed that the fluctuations in the upper atmosphere parameters with periods from a few days to a month observed from one point by ground-based instruments can be classified as traveling PWs.

This paper studies the PW effect on atmospheric temperature near the mesopause, using observations of the rotational temperature of OH (3-1) at two stations located approximately on the same meridian, but spaced in latitude. As an indicator of PW activity, the standard deviation of the average temperature is utilized after subtracting the seasonal component determined by the method proposed in [Bittner et al., 2002; Offermann et al., 2009]. This approach is distinguished by the simplicity of calculation; it is insensitive to the stationarity and linearity requirements, there is no need to calculate the period, amplitude, phase, and zonal wave number for each specific wave. This method has been adopted in [Perminov et al., 2014; Reisin et al., 2014].

INSTRUMENT AND METHOD

Two Shamrock spectrographs are installed at Maimaga station (63.04° N, 129.51° E) 150 km north of Yakutsk and at Tiksi high-latitude station (71.58° N, 128.77° E). The instrument at Maimaga station has been working since January 2013; and that at Tiksi station, since September 2015. For mutual calibration of the instruments, simultaneous observations were carried out for 10 days in August 2015. The software developed by SHICRA SB RAS allows the instruments to operate completely offline.

The spectrographs register the OH (3-1) band in the near infrared region (~1.5 μm) at a solar depression angle >9°. In this spectral region, the hydroxyl emission intensity is the highest, whereas the auroral emission intensity is much lower, as is the contribution of stray light from the Moon and stars, which decreases significantly — $1/\lambda^4$ times [Shefov et al., 2006]. The working cooling temperature of chambers of the spectrographs is set to –50° C to eliminate the temperature drift of the dark current; the exposure time is 60 s. Under these conditions, the spectrographs can measure the temperature in the mesopause region up to ~2 K (the error was calculated separately for each measurement).

The method of estimating the rotational molecular emission temperature involves fitting the model spectra, constructed taking into account the instrumental function for different preset temperatures, to the actually measured spectrum [Ammosov, Gavrilyeva, 2000; Gavrilyeva et al., 2021]. The OH(3-1) band is thermalized well enough, and the rotational temperature determined from it is close to the kinetic temperature of the surrounding neutral atmosphere at the height of its emission. When estimating the rotational temperature from the hydroxyl band, we have used the transition probabilities calculated in [Mies, 1974].

CALCULATION OF PLANETARY WAVE ACTIVITY AT DIFFERENT LATITUDES

The standard deviation σ_{pw} of the average overnight temperature T_{pw} (after subtracting seasonal variations f_{sv}) in the mesopause region from its monthly average value $T_{pw\text{-month\_av}}$ is taken as a characteristic of planetary wave activity:

$$\sigma_{pw} = \sqrt{\frac{\sum_{i=1}^{N}\left(T_{pw}^{i} - T_{pw\_month\_av}\right)^2}{N-1}},$$

where N is the number of measurements.

To account for the seasonal temperature variation, harmonics corresponding to its annual, semi-annual, and third-annual components are identified from average overnight temperatures:

$$f_{sv} = T_{year} + A_1\cos\left(\frac{2\pi}{365}(t-\varphi_1)\right) + $$
$$+A_2\cos\left(\frac{2\pi}{183}(t-\varphi_2)\right) + A_3\cos\left(\frac{2\pi}{122}(t-\varphi_3)\right).$$

Here T_{year} is the annual average temperature; A_1, A_2,A_3 are the amplitudes of annual/seasonal harmonics; t is the time (date, day of the year); φ is the corresponding time shift (given the phase).

The result of subtraction of the sum of seasonal variation harmonics from annual average overnight temperatures is consistent, as previously accepted, with the contribution of planetary wave propagation to the temperature (Figure 1).

Figures 2 and 3 present the results of calculation of seasonal variations and temperature disturbances caused by PW propagation for Maimaga and Tiksi stations respectively. There is a fairly clear pattern of the seasonal variation in the mesopause temperature measured at the two optical stations.

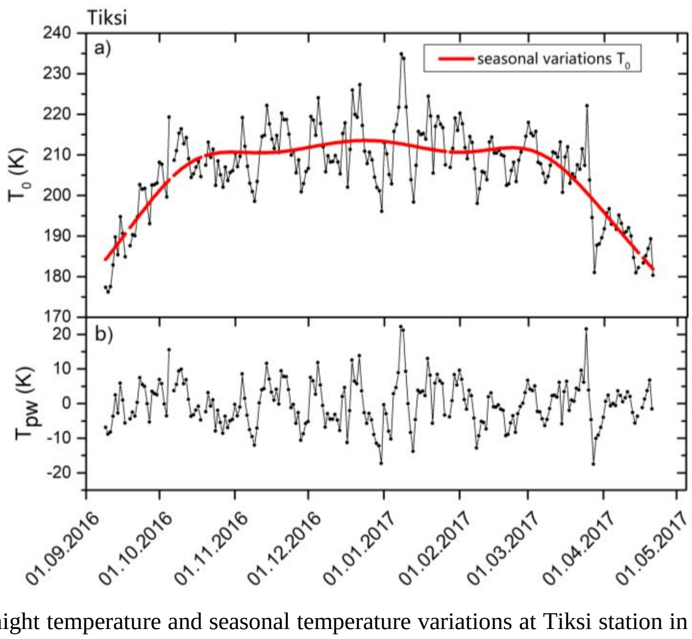

Figure 1. Average overnight temperature and seasonal temperature variations at Tiksi station in 2016–2017 (*a*). Temperature disturbances after subtracting the sum of seasonal variation harmonics (*b*)

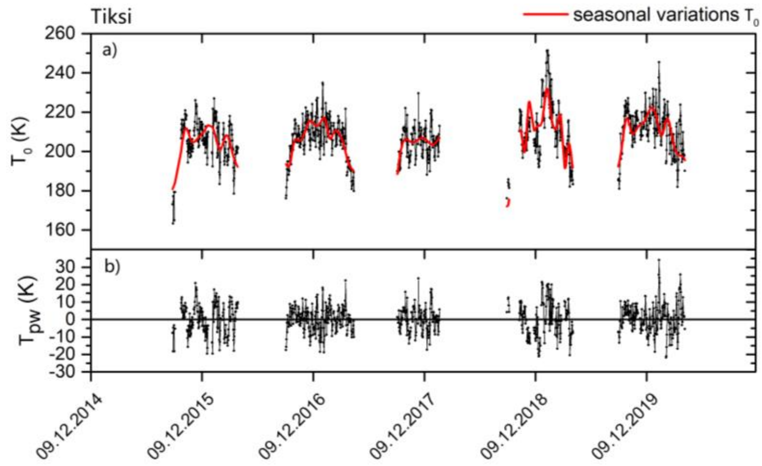

Figure 2. Average overnight temperature and seasonal temperature variations at the Maimaga station in 2013–2020 (*a*). Temperature disturbances after subtracting the sum of seasonal variation harmonics (*b*)

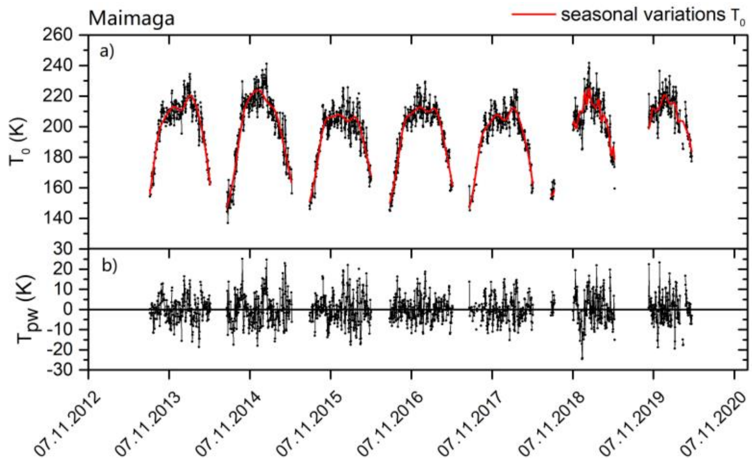

Figure 3. Average overnight temperature and seasonal temperature variations at Tiksi station in 2015–2020 (*a*). Temperature disturbances after subtracting the sum of seasonal variation harmonics (*b*)

Figures 4 and 5 show standard deviations of temperature σ_{pw} and relative standard deviations σ_{pw}/T_{month_av} from the monthly average values taken as characteristics of planetary wave activity. Errors in the determined temperature variability parameter (σ_{pw}) were calculated from the following formula [Atmosphere: handbook, 1991; Perminov et al., 2014]: $\delta_\sigma = \frac{\sigma}{\sqrt{2(n-1)}}$ is the error in determining the standard deviation, where n is the number of elements (measurements).

The relative standard deviations of temperature σ_{pw}/T_{month_av} obtained at Maimaga and Tiksi stations are close (~0.03) to σ_{dd}/T_0 from Zvenigorod station [Perminov et al., 2014]. To study interannual planetary wave activity, the standard deviations σ_{pw_year} of the dataset for one season were calculated without being subdivided by months. Annual activity σ_{pw_year} is the average planetary wave activity for one observation season (from September to May of each year). Annual planetary wave activity σ_{pw_year} for Maimaga and Tiksi stations is illustrated in Figure 6. Annual activity at Tiksi station exceeds that at Maimaga station by ~1.4 K in each individual season. In 2014–2015 and 2018–2019, there are peaks of annual activity σ_{pw_year} for Maimaga. In 2018–2019, annual activity σ_{pw_year} is also maximum for Tiksi. Figure 6 shows a tendency toward quasi-biennial fluctuations in activity, synchronous for both stations.

The same procedure as for calculation of σ_{pw} but without subdividing by months is used to calculate the standard deviation of the entire dataset. According to [Reisin et al., 2014], the resulting value is called the total value σ_{pw_total} (which does not exactly coincide with the mean for individual values of σ_{pw}) and, in fact, represents average planetary wave activity over all available calendar months.

The total planetary wave activity throughout the observation period σ_{pw_total} is 6.87±0.12 K for Maimaga and 8.25±0.20 K for Tiksi. Reisin et al. [2014] show total planetary wave activities in latitude for different stations around the world, with half of the data falling into a narrow range from 5.6 to 6.4 K. Yet, this does not exclude the existence of any latitude effect since all other high-latitude stations (Halley (75.52° S; 26.72° W), Rothera (67.57° S; 68.13° W), Stockholm (59.5° N; 18.2° E), Maimaga (63.1° N; 127.1° E), Longyearbyen (78.15° N; 16.04° E)), according to [Reisin et al., 2014], observe significantly higher planetary wave activity — ~8 K or higher. Planetary wave-induced disturbances of the average rotational temperature of hydroxyl after subtracting the seasonal variation as observed by Maimaga and Tiksi stations are displayed in Figure 7.

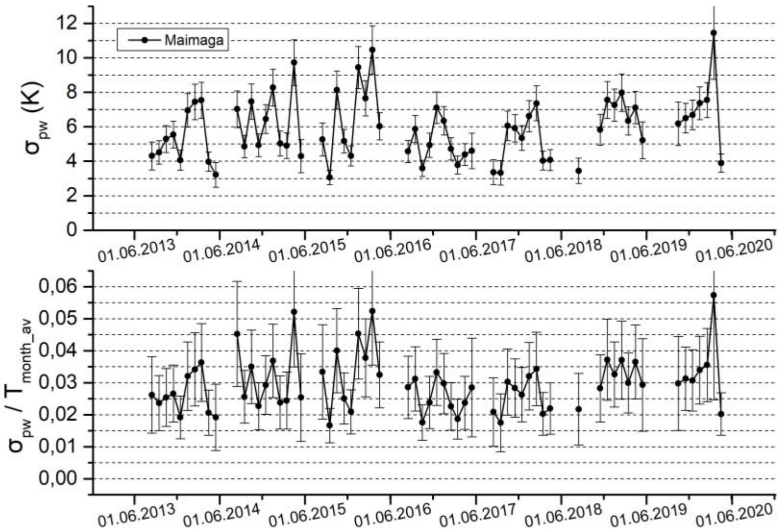

Figure 4. Standard deviations (*a*) and relative standard deviations of temperature (*b*) caused by planetary waves (2013–2020, Maimaga station)

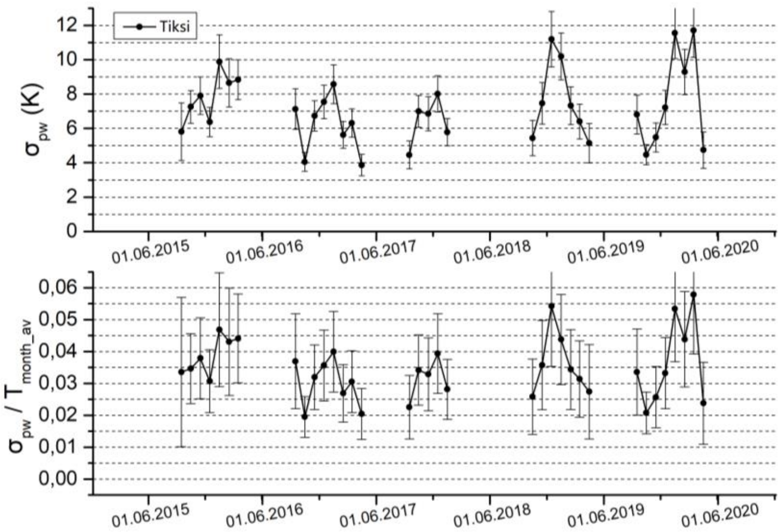

Figure 5. Standard deviations (*a*) and relative standard deviations of temperature (*b*) caused by planetary waves (2015–2020, Tiksi station)

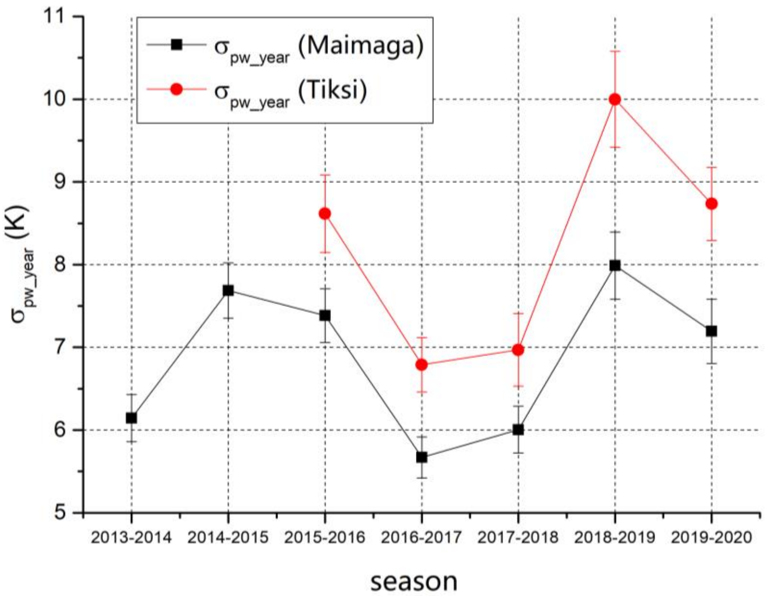

Figure 6. Annual planetary wave activity σ_{pw_year} for Maimaga and Tiksi stations (2013–2020)

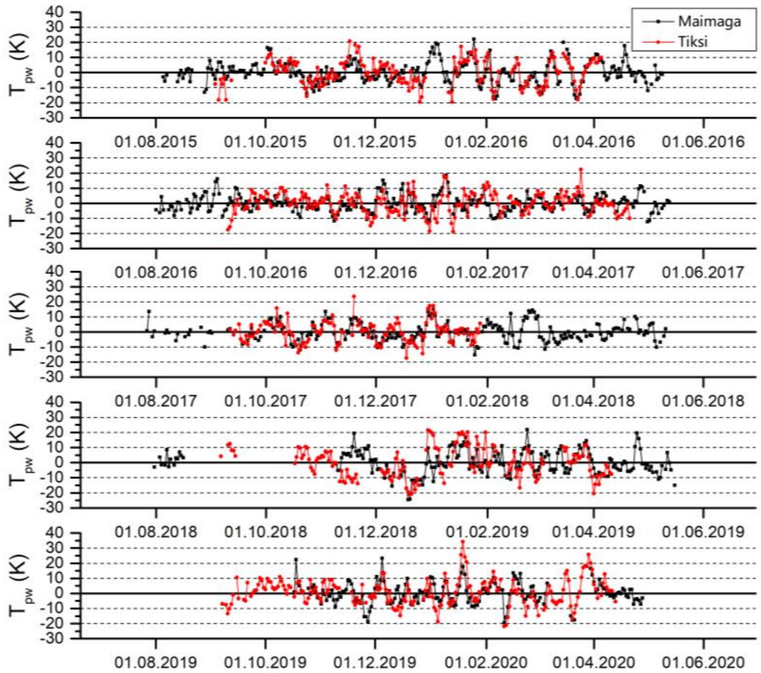

Figure 7. Temperature disturbances after subtracting the sum of seasonal variation harmonics at Maimaga and Tiksi stations in 2015–2020

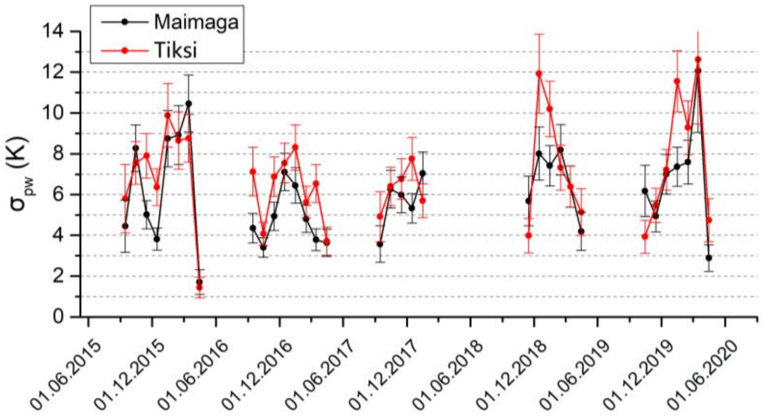

Figure 8. Standard temperature deviations caused by planetary waves at Maimaga and Tiksi stations in 2015–2020

Day-to-day fluctuations in the σ_{pw} dispersion occur synchronously at the optical stations, and at Tiksi station it is somewhat (by ~1–2 K) higher than at Maimaga station. The fact that the σ_{pw} fluctuations at the stations located approximately on the same meridian occur almost simultaneously is consistent with what is expected [Yiğit, Medvedev, 2015] and indicates predominantly zonal propagation of planetary waves at approximately the same phase velocity. Figure 8 exhibits planetary wave activity in 2015–2020 per month for the days on which simultaneous observations were carried out. Planetary wave activity at Tiksi station is by ~1.4 K higher than that at Maimaga station, i.e. it is higher at high latitudes.

This finding argues for the latitudinal dependence of planetary wave activity and is consistent with NDMC network observations [Reisin et al., 2014].

CONCLUSION

The behavior of the parameter σ_{pw} reflecting planetary wave activity at Maimaga and Tiksi stations in 2015–2020 has shown that σ_{pw} fluctuations at both stations occur almost synchronously, and in Tiksi it exceeds that in Maimaga. Planetary wave activity σ_{pw} in Tiksi is on average by 1–2 K higher than that in Maimaga. Annual planetary wave activity σ_{pw_year} in Tiksi exceeds that in Maimaga by ~1 K in each individual season. In 2014–2015 and 2018–2019, there are peaks of annual activity σ_{pw_year} for Maimaga. In 2018–2019, annual activity σ_{pw_year} was also maximum for Tiksi. The total planetary wave activity throughout the observation period σ_{pw_total} was 6.87±0.12 K in Maiymaga and 8.25±0.20 K in Tiksi. The results obtained indicate the latitudinal dependence of PW activity, which is consistent with the conclusions drawn from NDMC network observations. The simultaneous fluctuations in σ_{pw} recorded at the stations, located approximately on the same meridian, suggest predominantly zonal propagation of planetary waves with nearly the same phase velocity. The relative standard deviations of temperature σ_{pw}/T_{month_av} obtained at Maimaga and Tiksi stations are close (~0.03) to σ_{dd}/T_0 from Zvenigorod station [Perminov et al., 2014].

Organization, compilation, and accumulation of the data archive were financially supported by RSF No. 22-27-20137; statistical data processing, by RSF (Grant No. 22-77-1008); data analysis and interpretation, by Research and Educational Foundation for Support of Young Scientists of the Republic of Sakha (Yakutia), No. 1423122021 and under Government assignment (State Registration Number 122011700182-1).

REFERENCES

Atmosfera: spravochnik [Atmosphere: A handbook]. Leningrad, Gidrometeoizdat, 1991. 508 p. (In Russian).

Ammosov P.P., Gavrilyeva G.A. Infrared digital spectrograph for hydroxyl rotational temperature measurements. *Instruments and Experimental Techniques*. 2000, vol. 43, iss. 6, pp. 792–797.

Bittner M., Offermann D., Graef H.-H., Donner M., Hamilton K. An 18-year time series of OH rotational temperatures and middle atmosphere decadal variations. *J. Atmos. Solar-Terr. Phys.* 2002, vol. 64, iss. 8–11, pp. 1147–1166. DOI: 10.1016/S1364-6826(02)00065-2.

Gavrilyeva G.A., Ammosov P.P., Koltovskoi I.I., Sivtseva V.I., Iumshanov N.N. The optic meridional network in Yakutia: The method of mesopause temperature measurement. *AIP Confer. Proc.* 2021, voi. 2328, 050010. DOI: 10.1063/5.0042255.

Holton J.R., Haynes P.H., McIntyre M.E., Douglass A.R., Rood R.B., Pfister L. Stratosphere-troposphere exchange. *Rev. Geophys.* 1995, vol. 33, pp. 403–439. DOI: 10.1029/95RG02097.

Matsuno T. A dynamical model of the stratospheric sudden warming. *J. Atmos. Sci*. 1971, vol. 28, iss. 8, pp. 1479–1494. DOI: 10.1175/1520-0469(1971)028<1479:admots>2.0.co;2.

Mies F.H. Calculated vibrational transition probabilities of OH(X2Π). *J. Molec. Spectroscopy*. 1974, vol. 53, iss. 2, pp. 150–188. DOI: 10.1016/0022-2852(74)90125-8.

Offermann D., Gusev O., Donner M., Forbes J.M., Hagan M., Mlynczak M.G., et al. Relative intensities of middle atmosphere waves. *J. Geophys. Res*. 2009, vol. 114, D06110. DOI: 10.1029/2008JD010662.

Perminov V.I., Semenov A.I., Medvedeva I.V., Pertsev N.N. Temperature variations in the mesopause region according to the hydroxyl-emission observations at midlatitudes. *Geomagnetism and Aeronomy*. 2014, vol. 54, iss. 2, pp. 230–239. DOI: 10.1134/S0016793214020157.

Reisin E.R., Scheer J., Dyrland M.E., Sigernes F., Deehr C.S., Schmidt C., Hoppner K., et al. Traveling planetary wave activity from mesopause region airglow temperatures determined by the Network for the Detection of Mesospheric Change (NDMC). *J. Atmos. Solar-Terr. Phys.* 2014, vol. 119, pp. 71–82. DOI: 10.1016/j.jastp.2014.07.002.

Schoeberl M. Stratospheric warmings – observations and theory. *Rev. Geophys.* 1978, vol. 16, pp. 521–538. DOI: 10.1029/RG016i004p00521.

Shefov N.N., Semenov A.I., Khomich V.Yu. *Izluchenie verkhnei atmosfery — indikator ee struktury i dinamiki* [Airglow as an Indicator of the Upper Atmospheric Structure and Dynamics]. Moscow, GEOS Publ., 2006, 741 p. (In Russian).

Smith A. Global dynamics of the MLT. *Surv. Geophys*. 2012, vol. 33, pp. 1177–1230. DOI: 10.1007/s10712-012-9196-9.

Yiğit E., Medvedev A.S. Internal wave coupling processes in Earth's atmosphere. *Adv. Space Res*. 2015, vol. 55, iss. 4, pp. 983–1003. DOI: 10.1016/j.asr.2014.11.020.

Original Russian version: Sivtseva V.I., Ammosov P.P., Gavrilieva G.A., Ammosova A.M., Koltovskoi I.I., published in Solnechno-zemnaya fizika. 2022. Vol. 8. Iss. 4. P. 95–101. DOI: 10.12737/szf-84202209.

How to cite this article

Sivtseva V.I., Ammosov P.P., Gavrilieva G.A., Ammosova A.M., Koltovskoi I.I. Wave activity of the mesosphere in the planetary wave range according to OH (3-1) emission observations at Maimaga and Tiksi stations for 2015–2020. *Solar-Terrestrial Physics*. 2022. Vol. 8. Iss. 4. P. 89–94. DOI: 10.12737/stp-84202209.